Model for the ordered phases in KCN and NaCN

Harold T. Stokes and Dorian M. Hatch
Department of Physics and Astronomy, Brigham Young University, Provo, Utah 84602
(Received 5 March 1984)

We present, for KCN and NaCN in their electrically disordered and ordered low-temperature phases, a microscopic model using interatomic forces of the Born-Mayer type. We calculate with our model the atomic positions, the normal modes, and the elastic constants of KCN and NaCN in their ordered phase. We also calculate the atomic positions in the disordered phase. We adjust the parameters of our model to fit available experimental data. We then use this model to investigate other possible ordered structures of KCN and NaCN. Under the restriction that the order-disorder phase transition be continuous, we find that there are theoretically only six such structures. Using our model, we calculate the atomic positions as well as the energy per molecule for each of these structures. Our model predicts correctly which of these structures is most energetically favorable and should be experimentally observed.

I. INTRODUCTION

Both KCN and NaCN exhibit a continuous order-disorder phase transition in which the CN^- ions align themselves in an antiferroelectric manner. Considerable interest has been shown for this phase transition, as well as the structure and dynamics of the phases themselves. There have been experimental studies by dielectric response,[1,2] neutron scattering,[3–5] magnetic resonance,[6–10] elasticity measurements,[11] Raman spectroscopy,[12–15] and other optical techniques.[16–18] There have also been a number of theoretical studies.[19–25] We develop for KCN and NaCN a microscopic model using interatomic forces of the Born-Mayer type. We calculate with our model the atomic positions, the normal modes, and the elastic constants of KCN and NaCN in their antiferroelectric phase. We also calculate the atomic positions in the electrically disordered phase. We adjust the parameters of our model to fit available experimental data wherever possible.

We then use this model to investigate other possible ordered structures of KCN and NaCN. We consider ferroelectric as well as antiferroelectric ordering. Under the restriction that the order-disorder phase transition be continuous, we find there are theoretically only six such ordered structures. One of them is, of course, the antiferroelectric structure actually observed experimentally in KCN and NaCN. Using our model, we calculate the atomic positions as well as the energy per molecule for each of these six structures. Our model correctly predicts which of these structures is most energetically favorable and should be experimentally observed.

II. STRUCTURE

At room temperature both KCN and NaCN have a pseudocubic structure [phase I: space group O_h^5 ($Fm3m$), the NaCl structure] due to rapid reorientations of the CN^- ions which give them an effective average spherical shape. At 168 K in KCN and 288 K in NaCN, the crystals undergo a discontinuous transition[26–29] to an "elastically ordered" body-centered-orthorhombic structure [phase II: space group D_{2h}^{25} ($Immm$)]. In this phase, the CN^- ions are aligned parallel to the orthorhombic b axis (one of the cubic $\langle 110 \rangle$ directions in phase I), but are disordered with respect to their C and N ends. Since the CN^- ion carries a permanent electric dipole moment, this phase is sometimes called "electrically disordered." Rapid C-to-N reorientations of the CN^- ions maintain this disorder.

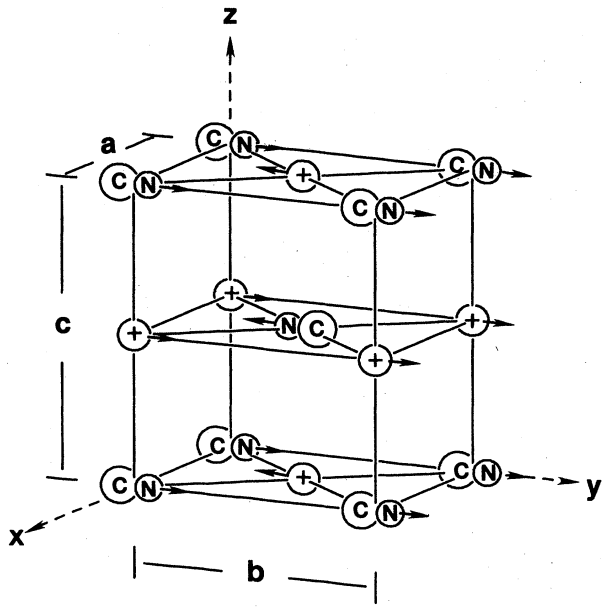

FIG. 1. Phase III of KCN and NaCN. The ions marked + are the K or Na ions. The direction of the displacements b_{anion} of the positive ions from their positions of symmetry are defined as shown by the arrows on the positive ions. The direction of the displacements b_{CN} of the CN^- centers of mass from their positions of symmetry are defined as shown by the arrows on the CN^- ions.

TABLE I. Atomic positions in a primitive unit cell of KCN and NaCN in phase III. There are two molecules per unit cell. The symbols a, b, and c are the orthorhombic lattice parameters, r_C and r_N are the distances of the C and N atoms, respectively, from the CN^- center of mass, and b_{CN} and b_{anion} are the displacements of the CN^- center of mass and the anion, respectively, from their sites of symmetry.

Atom	Positions [(x,y,z) coordinates]	
C	$(0,-r_C+b_{CN},0)$	$(\frac{1}{2}a,\frac{1}{2}b+r_C-b_{CN},\frac{1}{2}c)$
N	$(0,r_N+b_{CN},0)$	$(\frac{1}{2}a,\frac{1}{2}b-r_N-b_{CN},\frac{1}{2}c)$
K, Na	$(\frac{1}{2}a,\frac{1}{2}b-b_{anion},0)$	$(0,b_{anion},\frac{1}{2}c)$

At 83 K for KCN and 172 K for NaCN, the crystals undergo a *continuous* phase transition[3,4,28,29] to an antiferroelectric structure in which the CN^- ions are *ordered* with respect to C and N [phase III: space group D_{2h}^{13} (*Pmmn*)]. This phase is "electrically ordered." All CN^- ions in any given a-b plane are aligned parallel to each other, and CN^- ions in adjacent a-b planes are aligned antiparallel to each other (see Fig. 1). The Bravais lattice is primitive orthorhombic with two molecules per unit cell.

Using physical arguments, we can show that symmetry requires that the CN^- ordering be accompanied by ionic displacements in the $\pm b$ direction. We thus introduce the parameters, b_{anion} and b_{CN}, where b_{anion} is the displacement of the anions from their sites of symmetry, and b_{CN} is the displacement of the CN^- centers of mass from their sites of symmetry. We define the direction of these displacements as shown in Fig. 1. The atomic positions in the primitive unit cell for phase III are given in Tables I and II. We see that all like ions in a given a-b plane are displaced in the same direction, and like ions in adjacent a-b planes are displaced in opposite directions.

III. POSSIBLE STRUCTURES OF PHASE III

Let us now consider all the theoretically possible ordered structures of phase III which can theoretically arise from phase II via a continuous phase transition. The Landau theory[30] of continuous phase transitions places symmetry restrictions on the structure of the ordered phase. The direct group-theoretical conditions for this theory have recently been reformulated by Birman, Jarić, and others.[31–36] We restate them here briefly.

Consider a crystal with space-group symmetry G. A space group G' (a subgroup of G) is an allowed lower-symmetry space group for a continuous phase transition if the following criteria are met. G' must be associated with an irreducible representation (irrep) D of G such that the following is true.

(1) D subduces into the identity irrep of G' (subduction criterion).

(2) When G' is a subgroup of another subgroup, G'', of G, then the subduction frequency of G' must be greater than that of G'' (chain criterion). The subduction frequency of G' is the number of times that D subduces into the identity irrep of G'.

(3) The symmetrized triple Kronecker product of D does not contain the identity irrep of G (Landau criterion).

(4) The antisymmetrized double Kronecker product of D does not contain the vector representation of G (Lifshitz criterion).

Subgroups of G which satisfy the subduction and chain criteria are called isotropy groups of G.

An additional necessary physical condition requires that the free energy be a minimum (for the subgroup G') as the order parameter varies continuously from zero. We assume in the following that a range of coefficients in the free energy will allow all space groups satisfying conditions (1)–(4). Of course, this minimization should be specifically checked. The specific structure for KCN and NaCN and the model assumed in the following actually picks out the particular subgroup which minimizes the energy.

Irreps D of G are associated with points $\vec{k}$ in reciprocal space. The Lifshitz criterion can only be satisfied for an irrep D associated with a "point of symmetry" in reciprocal space. In our case, G is D_{2h}^{25}, the symmetry group of the disordered phase II. The lattice is body-centered orthorhombic. The points of symmetry in reciprocal space for this lattice are listed in Table III. We use Ref. 37 for the labeling and description of irreps. In addition, we use Ref. 38 for the basis vectors and origin of the space groups. For D_{2h}^{25}, all irreps associated with these points satisfy both the Landau and Lifshitz criteria except

TABLE II. Experimentally determined values of the parameters defined in Table I. Data is from neutron-scattering experiments of Fontaine (see Ref. 4).

	KCN (Å)	NaCN (Å)
a	4.20	3.63
b	5.26	4.85
c	6.09	5.45
r_C	0.65	0.65
r_N	0.55	0.55
b_{anion}	0.05	0.1
b_{CN}	0.04	0.00

TABLE III. Points of symmetry in reciprocal-lattice space for the body-centered-orthorhombic lattice. For the symbols we use the convention of Bradley and Cracknell (Ref. 37).

$\vec{k}$	(x,y,z) coordinates
Γ	$(0,0,0)$
X	$(0,0,2\pi/c)$
R	$(\pi/a,0,\pi/c)$
S	$(0,\pi/b,\pi/c)$
T	$(\pi/a,\pi/b,0)$
W	$(\pi/a,\pi/b,\pi/c)$

TABLE IV. Isotropy groups G' of D_{2h}^{25}. The labels of the irreps follow the convention of Bradley and Cracknell (Ref. 37). The quantity $i(G')$ is the subduction frequency of G', that is, the number of times that the irrep of G subduces into the density irrep of G'. The basis vectors listed are *conventional* basis vectors (not necessarily primitive) as given in Ref. 38. Note that for the base-centered monoclinic lattice, we use the first setting with the twofold axis along the c axis. The vectors listed under the "origin" column give the translation of the origin going from D_{2h}^{25} to G', using as origins the convention of Ref. 38 (the first settings). All vectors listed under the "basis vectors" and "origin" columns are given in terms of $\vec{a}$, $\vec{b}$, and $\vec{c}$ of the original orthorhombic lattice. The last column gives the CN^--site symmetry. The x, y, or z in parentheses gives the axis of the twofold rotation for the case of C_{2h}, C_{2v}, and C_2, and gives the direction normal to the plane of reflection for the case of C_{1h}. The structures possible for KCN and NaCN are marked with an asterisk (*).

$\vec{k}$	irrep	$i(G')$	G'	Basis vectors			Origin	CN^- site
Γ	Γ_1^+	1	D_{2h}^{25}	1,0,0	0,1,0	0,0,1	0,0,0	D_{2h}
	Γ_2^+	1	C_{2h}^3	$\bar{1}$,0,1	1,0,0	0,1,0	0,0,0	$C_{2h}(y)$
	Γ_3^+	1	C_{2h}^3	1,$\bar{1}$,0	0,1,0	0,0,1	0,0,0	$C_{2h}(z)$
	Γ_4^+	1	C_{2h}^3	0,1,$\bar{1}$	0,0,1	1,0,0	0,0,0	$C_{2h}(x)$
	Γ_1^-	1	D_2^8	1,0,0	0,1,0	0,0,1	0,0,0	D_2
	Γ_2^-	1	C_{2v}^{20}	0,0,1	1,0,0	0,1,0	0,0,0	$C_{2v}(y)$*
	Γ_3^-	1	C_{2v}^{20}	1,0,0	0,1,0	0,0,1	0,0,0	$C_{2v}(z)$
	Γ_4^-	1	C_{2v}^{20}	0,1,0	0,0,1	1,0,0	0,0,0	$C_{2v}(x)$
X	Γ_1^+	1	D_{2h}^1	1,0,0	0,1,0	0,0,1	0,0,0	D_{2h}
	Γ_2^+	1	D_{2h}^{12}	0,0,1	1,0,0	0,1,0	0,0,0	$C_{2h}(y)$
	Γ_3^+	1	D_{2h}^{12}	1,0,0	0,1,0	0,0,1	0,0,0	$C_{2h}(z)$
	Γ_4^+	1	D_{2h}^{12}	0,1,0	0,0,1	1,0,0	0,0,0	$C_{2h}(x)$
	Γ_1^-	1	D_{2h}^2	1,0,0	0,1,0	0,0,1	0,0,0	D_2
	Γ_2^-	1	D_{2h}^{13}	0,0,1	1,0,0	0,1,0	0,$\bar{\frac{1}{4}}$,0	$C_{2v}(y)$*
	Γ_3^-	1	D_{2h}^{13}	1,0,0	0,1,0	0,0,1	0,0,$\bar{\frac{1}{4}}$	$C_{2v}(z)$
	Γ_4^-	1	D_{2h}^{13}	0,1,0	0,0,1	1,0,0	$\bar{\frac{1}{4}}$,0,0	$C_{2v}(x)$
R	Γ_1^+	1	C_{2h}^3	$\bar{1}$,0,1	1,0,1	0,1,0	0,0,0	$C_{2h}(y)$
		1	D_{2h}^{19}	0,0,2	2,0,0	0,1,0	0,0,0	D_{2h}, $C_{2h}(y)$
		2	C_{2h}^1	$\bar{1}$,0,1	1,0,1	0,1,0	0,0,0	$C_{2h}(y)$
	Γ_2^+	1	C_{2h}^6	$\bar{1}$,0,1	1,0,1	0,1,0	$\frac{1}{4},\bar{\frac{1}{4}},\bar{\frac{1}{4}}$	C_i
		1	D_{2h}^{21}	0,0,2	2,0,0	0,1,0	$\bar{\frac{1}{2}}$,0,$\bar{\frac{1}{2}}$	$C_{2h}(x)$, $C_{2h}(z)$
		2	C_{2h}^4	$\bar{1}$,0,1	2,0,0	0,1,0	0,0,0	C_i
	Γ_1^-	1	C_{2h}^6	$\bar{1}$,0,1	1,0,1	0,1,0	$\bar{\frac{1}{4}},\bar{\frac{1}{4}},\bar{\frac{1}{4}}$	$C_2(y)$*
		1	D_{2h}^{21}	0,0,2	2,0,0	0,1,0	0,0,$\bar{\frac{1}{2}}$	D_2, $C_{2v}(y)$
		2	C_{2h}^4	$\bar{1}$,0,1	2,0,0	0,1,0	$\bar{\frac{1}{2}}$,0,0	$C_2(y)$
	Γ_2^-	1	C_{2h}^3	$\bar{1}$,0,1	1,0,1	0,1,0	0,0,$\bar{\frac{1}{2}}$	$C_{1h}(y)$
		1	D_{2h}^{19}	0,0,2	2,0,0	0,1,0	$\bar{\frac{1}{2}}$,0,0	$C_{2v}(x)$, $C_{2v}(z)$
		2	C_{2h}^1	$\bar{1}$,0,1	1,0,1	0,1,0	0,0,$\bar{\frac{1}{2}}$	$C_{1h}(y)$
S	Γ_1^+	1	C_{2h}^3	0,1,$\bar{1}$	0,1,1	1,0,0	0,0,0	$C_{2h}(x)$
		1	D_{2h}^{19}	0,2,0	0,0,2	1,0,0	0,0,0	D_{2h}, $C_{2h}(x)$
		2	C_{2h}^1	0,1,1	0,$\bar{1}$,1	1,0,0	0,0,0	$C_{2h}(x)$
	Γ_2^+	1	C_{2h}^6	0,1,$\bar{1}$	0,1,1	1,0,0	$\bar{\frac{1}{4}},\bar{\frac{1}{4}},\frac{1}{4}$	C_i
		1	D_{2h}^{21}	0,2,0	0,0,2	1,0,0	0,0,0	$C_{2h}(y)$, $C_{2h}(z)$

TABLE IV. (*Continued*).

$\vec{k}$	irrep	$i(G')$	G'	Basis vectors			Origin	CN^- site
		2	C_{2h}^4	0,1,$\bar{1}$	0,0,2	1,0,0	0,0,0	C_i
	Γ_1^-	1	C_{2h}^6	0,1,$\bar{1}$	0,1,1	1,0,0	$\frac{1}{4},\frac{\bar{1}}{4},\frac{1}{4}$	$C_2(x)$
		1	D_{2h}^{21}	0,2,0	0,0,2	1,0,0	$0,\frac{\bar{1}}{2},0$	D_2, $C_{2v}(x)$
		2	C_{2h}^4	0,1,$\bar{1}$	0,0,2	1,0,0	$0,0,\frac{\bar{1}}{2}$	$C_2(x)$
	Γ_2^-	1	C_{2h}^3	0,1,$\bar{1}$	0,1,1	1,0,0	$0,\frac{\bar{1}}{2},0$	$C_{1h}(x)$*
		1	D_{2h}^{19}	0,2,0	0,0,2	1,0,0	$0,\frac{\bar{1}}{2},0$	$C_{2v}(y)$, $C_{2v}(z)$
		2	C_{2h}^1	0,1,1	0,$\bar{1}$,1	1,0,0	$0,0,\frac{\bar{1}}{2}$	$C_{1h}(x)$
T	Γ_1^+	1	C_{2h}^3	1,$\bar{1}$,0	1,1,0	0,0,1	0,0,0	$C_{2h}(z)$
		1	D_{2h}^{19}	2,0,0	0,2,0	0,0,1	0,0,0	D_{2h}, $C_{2h}(z)$
		2	C_{2h}^1	1,1,0	$\bar{1}$,1,0	0,0,1	0,0,0	$C_{2h}(z)$
	Γ_2^+	1	C_{2h}^6	1,$\bar{1}$,0	1,1,0	0,0,1	$\frac{\bar{1}}{4},\frac{1}{4},\frac{\bar{1}}{4}$	C_i
		1	D_{2h}^{21}	2,0,0	0,2,0	0,0,1	0,0,0	$C_{2h}(x)$, $C_{2h}(y)$
		2	C_{2h}^4	1,$\bar{1}$,0	0,2,0	0,0,1	0,0,0	C_i
	Γ_1^-	1	C_{2h}^6	1,$\bar{1}$,0	1,1,0	0,0,1	$\frac{\bar{1}}{4},\frac{1}{4},\frac{\bar{1}}{4}$	$C_2(z)$
		1	D_{2h}^{21}	2,0,0	0,2,0	0,0,1	$\frac{\bar{1}}{2},0,0$	D_2, $C_{2v}(z)$
		2	C_{2h}^4	1,$\bar{1}$,0	0,2,0	0,0,1	$0,\frac{\bar{1}}{2},0$	$C_2(z)$
	Γ_2^-	1	C_{2h}^3	1,$\bar{1}$,0	1,1,0	0,0,1	$\frac{\bar{1}}{2},0,0$	$C_{1h}(z)$*
		1	D_{2h}^{19}	2,0,0	0,2,0	0,0,1	$\frac{\bar{1}}{2},0,0$	$C_{2v}(x)$, $C_{2v}(y)$
		2	C_{2h}^1	1,1,0	$\bar{1}$,1,0	0,0,1	$0,\frac{\bar{1}}{2},0$	$C_{1h}(z)$
W	Γ_1	1	D_{2h}^{23}	0,2,0	0,0,2	2,0,0	0,0,0	D_{2h}, D_2
		1	D_{2h}^{24}	2,0,0	0,2,0	0,0,2	0,0,0	D_2
		2	D_2^7	0,2,0	0,0,2	2,0,0	0,0,0	D_2
	Γ_2	1	D_{2h}^{23}	0,2,0	0,0,2	2,0,0	$0,\frac{\bar{1}}{2},0$	$C_{2h}(y)$, $C_{2v}(y)$
		1	D_{2h}^{24}	2,0,0	0,2,0	0,0,2	$0,\frac{\bar{1}}{2},0$	$C_2(y)$*
		2	D_2^7	0,2,0	0,0,2	2,0,0	$0,\frac{\bar{1}}{2},0$	$C_2(y)$
	Γ_3	1	D_{2h}^{23}	0,2,0	0,0,2	2,0,0	$0,0,\frac{\bar{1}}{2}$	$C_{2h}(z)$, $C_{2v}(z)$
		1	D_{2h}^{24}	2,0,0	0,2,0	0,0,2	$0,0,\frac{\bar{1}}{2}$	$C_2(z)$
		2	D_2^7	0,2,0	0,0,2	2,0,0	$0,0,\frac{\bar{1}}{2}$	$C_2(z)$
	Γ_4	1	D_{2h}^{23}	0,2,0	0,0,2	2,0,0	$\frac{\bar{1}}{2},0,0$	$C_{2h}(x)$, $C_{2v}(x)$
		1	D_{2h}^{24}	2,0,0	0,2,0	0,0,2	$\frac{\bar{1}}{2}0,0$	$C_2(x)$
		2	D_2^7	0,2,0	0,0,2	2,0,0	$\frac{\bar{1}}{2},0,0$	$C_2(x)$

for the identity irrep (irrep Γ_1^+ of the Γ point).

Applying the subduction and chain criteria to all subgroups of D_{2h}^{25}, we obtain all the isotropy groups and list them in Table IV. (More details about the generation of this list will be given in a separate publication.) Crystals with a structure of symmetry D_{2h}^{25} may theoretically exhibit a continuous phase transition to any of these isotropy groups (for the isotropy group D_{2h}^{25} of the identity irrep, of course, there is no transition). However, if we consider a *specific* crystal of symmetry D_{2h}^{25}, we will find that only a small number of these isotropy groups actually describe a physically possible lower-symmetry structure of that crystal.

In particular, for KCN and NaCN we place two requirements on the structure of phase III. First, the C and N ends of the CN^- ions should be distinguishable. We

TABLE V. Allowed point symmetries of CN^- site in the ordered structure of phase III. The x, y, or z in parentheses has the same meaning as in Table IV.

Point symmetry	Point operators
$C_{2v}(y)$	E, C_{2y}, σ_x, σ_z
$C_2(y)$	E, C_{2y}
$C_{1h}(x)$	E, σ_x
$C_{1h}(z)$	E, σ_z
C_1	E

want the phase transition to be of the order-disorder type. Second, the CN^- should be still aligned along the general direction of the b axis of phase II. We are not looking for phase transitions where the CN^-'s end up pointing along the a or the c axis. This change would be nonphysical.

The point symmetry of the CN^- site in phase II is D_{2h}, which contains the point-group operations E, C_{2x}, C_{2y}, C_{2z}, I, σ_x, σ_y, and σ_z. If we apply the two requirements we place on phase III, the point symmetry of the CN^- site in phase III *cannot* include I, σ_y, C_{2x}, or C_{2z}. Using the remaining four point-group operations in D_{2h}, we can construct four point groups. These are listed in Table V. The point symmetry of the CN^- site in phase III must belong to one of these point groups.

In Table IV we show, for each isotropy group, the point symmetry of the CN^- site. Some structures actually divide the CN^- sites into two different kinds of sites with different point symmetries, as indicated in the table. As can be seen, there are only 10 isotropy groups in which each CN^- site has one of the allowed point symmetries listed in Table V. However, we need to eliminate even some of these from further consideration. For example, irrep Γ_1^- of the R point gives rise to two isotropy groups, C_{2h}^6 and C_{2h}^4, with a CN^- site symmetry of $C_2(y)$. Both of these structures exhibit the *identical* CN^- ordering (that is, the orientation of the C and N ends of the CN^- ions are the same). In fact, we find that C_{2h}^4 is a subgroup of C_{2h}^6. The C_{2h}^4 structure has *less* symmetry than the C_{2h}^6 structure. In the transition from phase II, a certain amount of symmetry is lost just from the ordering of the CN^- ions alone. This brings us to a structure of symmetry C_{2h}^6. Additional symmetry must be lost to bring us to a structure of symmetry C_{2h}^4. This must be accomplished through some further structural change *beyond* the CN^- ordering. For example, if some of the CN^- ions were displaced along the b axis by an amount slightly different from other CN^- ions, we could obtain a structure of symmetry C_{2h}^4.

We eliminate the C_{2h}^4 structure from further consideration for the following two reasons. First, continuous phase transitions from a space group G take us to maximal subgroups[39] of G. We know of only one example[40] (and it is a model) which does not follow this rule. Second, the interatomic forces we use in our microscopic model cannot produce a C_{2h}^4 structure. For the same reasons, we also eliminate from further consideration the C_{2h}^1 group for both the irrep Γ_2^- of the S point and the irrep Γ_2^- of the T point, and the D_2^7 group for the irrep Γ_2 of the W point. This leaves us with six isotropy groups,

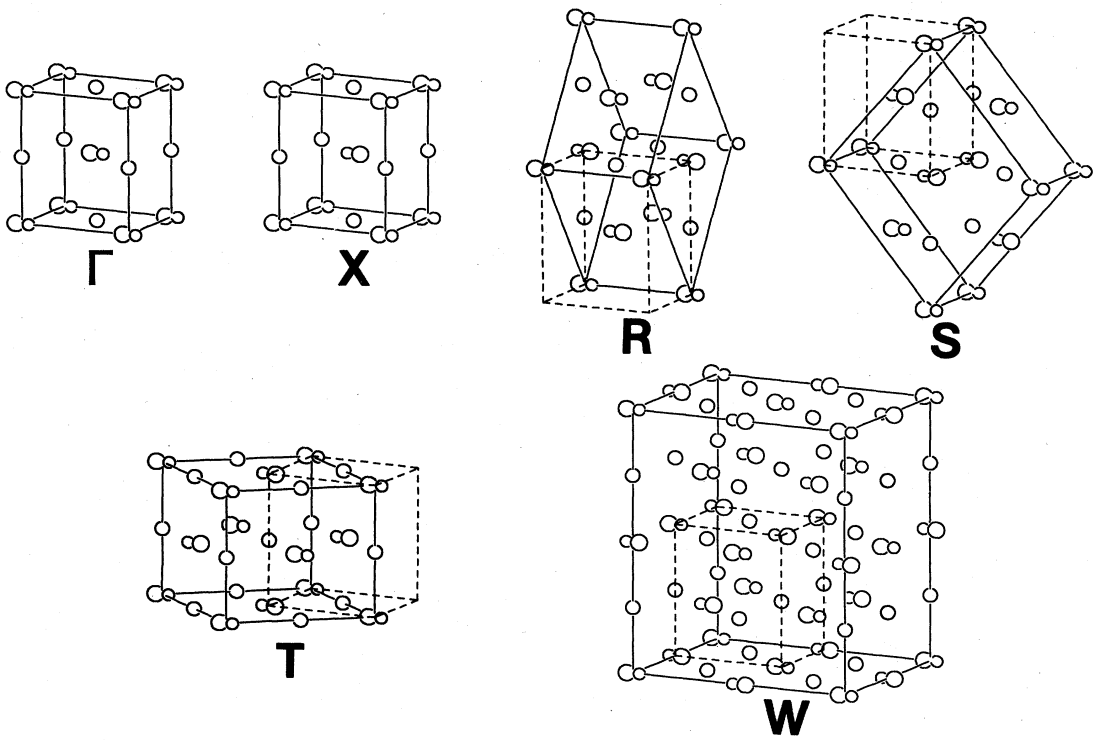

FIG. 2. Six possible ordered structures of KCN and NaCN given in Table VI. Dashed lines show the original unit cell, and solid lines show the new unit cell. (The unit cells shown are conventional and not necessarily primitive.)

TABLE VI. Possible structures of KCN and NaCN in phase III. The point symmetry of the CN^- site in each structure is also given. The x, y, or z in parentheses has the same meaning as in Table IV. These structures are marked with an asterisk (*) in Table IV.

$\vec{k}$	G'	Bravais lattice	CN^- site
Γ	C_{2v}^{20}	body-centered orthorhombic	$C_{2v}(y)$
X	D_{2h}^{13}	primitive orthorhombic	$C_{2v}(y)$
R	C_{2h}^{6}	base-centered monoclinic	$C_2(y)$
S	C_{2h}^{3}	base-centered monoclinic	$C_{1h}(x)$
T	C_{2h}^{3}	base-centered monoclinic	$C_{1h}(z)$
W	D_{2h}^{24}	face-centered orthorhombic	$C_2(y)$

one for each $\vec{k}$. These are listed in Table VI. Their structures are shown in Fig. 2. For the remainder of this paper we will refer to these groups as simply the Γ structure, X structure, etc.

The Bravais lattices for each of these structures are given by all points $\vec{t}$ in the original body-centered-orthorhombic lattice of phase II which satisfy $\exp(-i\vec{k}\cdot\vec{t})=1$. Let us place a lattice point at one of the CN^- ions. All the CN^- ions which fall on the other lattice points are at equivalent positions and are thus aligned in the same direction. If there is more than one CN^- ion in the primitive unit cell, their relative orientations can be found from the symmetry operations of the space group. In the Γ structure ($\vec{k}=0$), all the CN^- ions fall on lattice points, and the structure is ferroelectric. In the X, R, S, and T structures, only half of the CN^- ions fall on lattice points. The other half are aligned in the opposite direction, and these structures are antiferroelectric. In the W structure, only a fourth of the CN^- ions fall on lattice points. The size of the primitive unit cell is quadrupled. From the symmetry operations of D_{2h}^{24}, we find that there are two equivalent ways to order the CN^- ions within the unit cell. We choose the following. Those CN^- ions at sites $\vec{t}$ for which $\exp(-i\vec{k}\cdot\vec{t})=1$ or $\exp(-i\vec{k}\cdot\vec{t})=i$ are aligned in one direction and the rest are aligned in the opposite direction. The W structure is thus antiferroelectric.

IV. PREVIOUS MODELS

A. Ising model

One of the simplest models for KCN and NaCN in phases II and III is the Ising model. Each CN^- ion possesses a permanent electric dipole moment. Furthermore, the CN^- ions are constrained to point either parallel or antiparallel to the b axis. The dipole-dipole energy of such a system may be written as

$$U=-\tfrac{1}{2}\sum_{\substack{i,j\\ i\neq j}} J_{ij}S_iS_j\ , \tag{1}$$

where the summation is over all CN^- ions in the crystal. The "Ising spin" S_i is a number equal to ±1 and indicates the direction of the CN^- ion at site i. The dipole $\vec{p}_i$ at site i is thus given by

$$\vec{p}_i=S_ip\hat{b}\ , \tag{2}$$

where p is the permanent electric dipole moment of the CN^- ion and $\hat{b}$ is a unit vector along the b axis. The coupling parameter J_{ij} in Eq. (1) is given by

$$J_{ij}=p^2r_{ij}^{-3}(3\cos^2\theta_{ij}-1)\ , \tag{3}$$

where $\vec{r}_{ij}$ is a vector from site i to site j, and θ_{ij} is the angle between $\vec{r}_{ij}$ and the b axis.

For a structure with dipole ordering, we obtain from Eq. (1) the energy per molecule,

$$\frac{U}{N}=-\tfrac{1}{2}\sum_{\substack{j\\ i\neq j}} J_{ij}S_iS_j\ . \tag{4}$$

We have evaluated this expression for all six possible ordered structures in KCN and NaCN (see Table VII). In each case, we summed over sites j in an orthorhombic volume of dimensions $10a\times10b\times10c$ centered on site i. Our results are similar to those of dos Santos *et al.*,[19] who performed the same calculation for five of these structures in KCN. [Note that their values are approximately twice as large as ours since they evaluated the energy per dipole *pair* and did not include the factor $\frac{1}{2}$ as we did in Eq. (4). A residual discrepancy in values arises from a slightly different choice of lattice parameters a, b, and c. We used the values shown in Table II.]

For the ferroelectric Γ structure, a correction to U/N must be made because of the charge density at the boundary of the volume where the summation is performed.[41,19] In this case the crystal has a net macroscopic polarization P which produces a surface charge density $\sigma=\pm P$ on the two ends of the orthorhombic volume which are normal to the b axis. This produces at site i an electric field E given by

TABLE VII. Relative energy per molecule for the possible ordered structures of KCN and NaCN using the Ising model.

$\vec{k}$	KCN U/Np^2 (10^{-4} Å^{-3})	NaCN U/Np^2 (10^{-4} Å^{-3})
Γ	−269	−361
X	29	102
R	−207	−286
S	220	315
T	−28	−81
W	−53	−111

$$E = 8P \tan^{-1}\left[\frac{ac}{b(a^2+b^2+c^2)^{1/2}}\right], \quad (5)$$

which is independent of the volume size (but, of course, *not* independent of the volume *shape*). The correction to U/N is given by $\Delta U/N = -\frac{1}{2}pE$ [the factor $\frac{1}{2}$ is again included, as in Eq. (4), to give us energy per molecule], and, using $P = 2p/abc$ (two CN^- ions per volume abc), we obtain

$$\Delta U/N = -\frac{8p^2}{abc}\tan^{-1}\left[\frac{ac}{b(a^2+b^2c^2)^{1/2}}\right]. \quad (6)$$

With this correction, the ferroelectric Γ structure has the lowest energy of any of the other structures listed in Table VII. Since the antiferroelectric X structure is the one experimentally observed for both KCN and NaCN at low temperatures, we would expect a *good* model to yield the *lowest* energy for that structure. Instead, the Ising model yields lower energies for the ferroelectric Γ structure as well as three other antiferroelectric structures, R, T, and W. There are obviously some serious flaws in the Ising model as applied to KCN and NaCN.

B. Induced dipoles

Pirc and Vilfan[23] improved on the Ising model for KCN and NaCN by allowing the lattice to be deformable. Displacements of the ions from their sites of symmetry produce induced dipoles which must then be included in the dipole-dipole energy given by Eq. (1). Pirc and Vilfan effectively calculated the relative size of these displacements, using estimates of the frequencies of the phonon modes involved, and were thus able to obtain the relative dipole energies of four ordered structures (Γ, X, R, T). Of these four, they found that the X structure has the lowest energy, which, of course, agrees with the experimental result. Recently, Koiller *et al.*[24] also introduced a simple model where induced dipoles are placed at the positive-ion sites. They likewise showed that the resulting dipolar energy greatly favors the X structure.

It is simple to understand how induced dipoles, particularly at the positive-ion sites, can have such a large effect on the total dipole energy. Consider, for example, the X structure. In this structure, the positive ions (K or Na) are displaced such that their induced dipole moments point in the same direction as the permanent dipole moments of their neighboring CN^- ions in the same a-b plane. Thus, all dipoles, permanent and induced, in the same a-b plane, are parallel to each other, whereas dipoles in adjacent a-b planes are antiparallel (see Fig. 3).

Now consider two nearest-neighbor CN^- ions such as those at (0,0,0) and $(\frac{1}{2}a, \frac{1}{2}b, \frac{1}{2}c)$. In the X structure they are aligned antiparallel. Unaided by induced dipoles, their energy of interaction, given by Eq. (3), is very weak (the factor $3\cos^2\theta - 1$ is nearly zero). Neither parallel nor antiparallel alignment is appreciably favored. However, the induced dipole at the positive-ion site $(\frac{1}{2}a, \frac{1}{2}b, 0)$ is aligned parallel to the CN^- at (0,0,0) and antiparallel to the CN^- at $(\frac{1}{2}a, \frac{1}{2}b, \frac{1}{2}c)$. Both of these alignments are strongly favored by the dipole-dipole interaction, resulting in an indirect interaction between the two CN^- ions which favors antiparallel alignment. We obtain a similar result using the induced dipole at the positive-ion site $(0,0,\frac{1}{2}c)$.

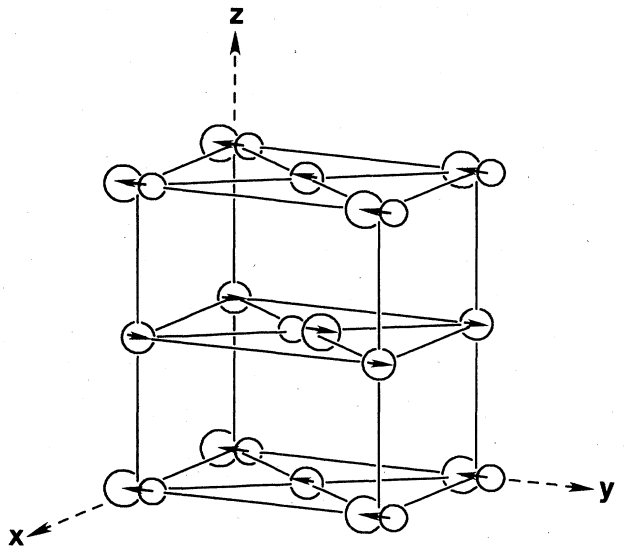

FIG. 3. Permanent and induced electric dipoles in phase III of KCN and NaCN. The arrows indicate the direction of the dipoles. The identity of the atoms are the same as that shown in Fig. 1.

As a second example, consider the two next-nearest-neighbor CN^- ions at (0,0,0) and $(0,0,c)$. In the X structure, they are aligned parallel. Unaided by induced dipoles, their energy of interaction favors antiparallel alignment. However, the induced dipole at the positive-ion site $(0,0,\frac{1}{2}c)$ directly between the two CN^- ions is aligned antiparallel to each CN^- ion. Both of these alignments are strongly favored, leading to an effective interaction between the two CN^- ions which favors *parallel* instead of antiparallel alignment.

From these examples, we can see how the presence of induced dipoles lowers the energy of the X structure. The other structures are not as greatly aided by induced dipoles in the ways we have seen above for the X structure. In the R structure, for example, the positive ions are constrained by symmetry to have *zero* displacement, thus producing *no* induced dipoles. Allowing the lattice to be deformable greatly favors the X structure relative to the others and constitutes the principle reason this structure is the one observed in nature.

V. OUR MODEL

A. Interatomic forces

The model we have chosen to represent KCN and NaCN is an atomic model which explicitly gives the interionic forces. Since this model allows lattice deformations, it contains the feature which made the model of Pirc and Vilfan so successful (discussed in Sec. IV B). Furthermore, as we shall see, our model allows us to investigate other interesting properties of KCN and NaCN

in addition to just the energies of different dipolar configurations.

Our model initially contained two different kinds of interionic interactions: long-ranged electrostatic and short-ranged repulsive. The electrostatic energy is given by the sum over the Coulomb energy U_{ij} between pairs of point charges q_i and q_j:

$$U_{ij}=q_iq_j/r_{ij}\ , \tag{7}$$

where $\vec{r}_{ij}$ is the vector from q_i to q_j.

In our model we place a positive point charge at the nucleus of each positive ion, and we place three point charges on each CN^- ion (which we treat as a rigid dumbbell): a point charge q_C at the C nucleus, a point charge q_N at the N nucleus, and a point charge $q_{c.m.}$ at the CN^- center of mass. With three charges on the CN^- ion, we can independently adjust its total charge $q_0=q_C+q_N+q_{c.m.}$ (we must simultaneously adjust the charge on the positive ion to maintain the electric neutrality of the crystal), its electric dipole moment $p=r_Cq_C-r_Nq_N$, and its electric quadrupole moment $Q=2(r_C^2q_C+r_N^2q_N)$, where r_C and r_N are the distances from the CN^- center of mass to the C and N nuclei, respectively. The moments p and Q are taken about the CN^- center of mass.

The short-ranged repulsive interaction between ions is of the Born-Mayer type,[42]

$$U_{ij}=\lambda_{ij}\exp\left[-\frac{r_{ij}}{\rho_{ij}}\right], \tag{8}$$

where r_{ij} is the distance between atomic nuclei. The energy U_{ij} is a rather steep function of r_{ij}, and the atoms almost behave like hard spheres. This model is sometimes called the "soft-sphere" model.[43]

For the case of interactions between like atoms, we find approximate values for λ_{ij} and ρ_{ij} in the literature,[42,44,45] as shown in Table VIII. These values were obtained by fitting the Born-Mayer model to various crystal structures containing K, Na, C, and N atoms. Values for λ_{ij} and ρ_{ij} between *unlike* atoms can be obtained by simple empirical relationships,[45,46]

$$\lambda(A,B)=[\lambda(A,A)\lambda(B,B)]^{1/2} \tag{9}$$

and

$$\frac{1}{\rho(A,B)}=\frac{1}{2}\left[\frac{1}{\rho(A,A)}+\frac{1}{\rho(B,B)}\right], \tag{10}$$

where $\lambda(A,B)$ and $\rho(A,B)$ refer to the interaction between an atom of type A and an atom of type B.

The total energy of the crystal is given by

$$U=\tfrac{1}{2}\sum_{\substack{i,j\\ i\neq j}}\frac{q_iq_j}{r_{ij}}+\tfrac{1}{2}\sum_{\substack{i,j\\ i\neq j}}\lambda_{ij}\exp\left[-\frac{r_{ij}}{\rho_{ij}}\right]. \tag{11}$$

In the first term the summation over j for a fixed i is performed over an orthorhombic volume of dimensions $4a\times4b\times4c$ centered on site i. The method of Evjen[47] is used where charges of ions at the boundary of the volume are reduced by some factor in order to ensure zero net charge within the volume and zero net charge on each face of the boundary. (Specifically, charges on faces are divided by 2, those on edges by 4, and those on corners by 8.) In the second term of Eq. (11), the summation over j for a fixed i is performed over the six nearest unlike neighboring ions and the eight nearest like neighboring ions.

To find the structure and energy of the crystal using our model, we allow the ions to "relax." We adjust their positions such that the net force (and the net torque for the case of CN^-) on each ion is zero and that the pressure is zero (i.e., the lattice is stable against volume expansion or contraction). This condition is achieved by minimizing U with respect to the lattice constants (a,b,c) and the positions of the ions within the unit cell. In the case of phase III in KCN and NaCN (the X structure), only two parameters, b_{anion} and b_{CN}, are needed to specify the positions of the ions within the unit cell (see Sec. II). Thus, we require

$$\frac{\partial U}{\partial a}=\frac{\partial U}{\partial b}=\frac{\partial U}{\partial c}=\frac{\partial U}{\partial b_{anion}}=\frac{\partial U}{\partial b_{CN}}=0\ . \tag{12}$$

For a given configuration of ions (i.e., their positions and orientations), the forces between them depend only on our choice of charge distribution (q_0,p,Q) and the Born-Mayer parameters (λ_{ij},ρ_{ij}). We call these the "force parameters." Once we specify a choice of values for the force parameters, we can use the five simultaneous equations in Eq. (12) to determine the "structure parameters," which, in this case, are a, b, c, b_{anion}, and b_{CN}. (We do this numerically, using the Newton-Raphson method.[48]) Actually, what we need to do is solve the inverse problem. We know the structure parameters. We want to determine

TABLE VIII. Born-Mayer parameters for the interatomic repulsive force. The values of these parameters from the literature were obtained by best fits to experimental data for the crystals listed.

Atom	λ_{ii} (10^{-8} erg)	ρ_{ii} (Å)	Crystal	Ref.
		From literature		
K	0.2201	0.3394	alkali halides	42
Na	0.0410	0.3394	alkali halides	42
C	0.498	0.272	naphthalene	44
N	0.292	0.265	NO_2	45
		Present work		
K	0.2201	0.3394		
Na	0.0410	0.3394		
C	0.381	0.268		
N	0.381	0.268		

the force parameters which give us the known structure. We do this by starting with a "reasonable" set of values for the force parameters, and then adjust some of their values such that the solution to Eq. (12) gives us the desired structure parameters.

Using this approach, we were able to obtain the experimentally obtained values of a, b, and c by adjusting *three* force parameters: (1) the total charge q_0 of the CN^- ion, (2) the electric quadrupole moment Q of the CN^- ion, and (3) the value of λ_{ij} between nearest-neighbor ions along the c direction. Furthermore, we found that we could obtain *nearly* the desired values of a, b, and c, for both KCN and NaCN by using the *same* adjustments in these parameters for both crystals. The result is shown in Table IX.

Let us summarize here the values of the force parameters which we used. For the charge distribution on the CN^- ion, we used $q_0=-0.89e$, $p/e=0.11$ Å, and $Q/e=-1.7$ Å^2, where e is the magnitude of the electronic charge. As mentioned above, q_0 and Q were adjusted to give the best values for a, b, and c. Our value for q_0 could be physically interpreted to indicate an incomplete charge transfer from the positive ions to the CN^- ions (i.e., these crystals are not 100% ionic). Our choice for p is discussed in Sec. V D. The value for Q in a *free* CN^- ion has been theoretically calculated by Gready *et al.*[49] using the finite-field method. They obtained $Q/e=-1.0$ Å^2, which is much smaller than our value. This is a bit disturbing since others[50,46] have stated that the value of Q for CN^- in a crystal should be *less* than its free-ion value. However, our large value of Q was absolutely essential in order to obtain the correct ratio a/b. No adjustment of any other force parameter could achieve this. However, since this *is* only a model, perhaps we should not attach any physical significance to our large value of Q.

For the Born-Mayer parameters we used the values from the literature (see Table VIII) with two modifications. First, we used "average" values for λ(C,C) and λ(N,N) and for ρ(C,C) and ρ(N,N) such that λ(C,C)=λ(N,N) and ρ(C,C)=ρ(N,N), as shown in Table VIII. The reasons for this choice are discussed below. The values for λ_{ij} and ρ_{ij} between unlike atoms were obtained from Eqs. (9) and (10).

Second, we reduced, by a factor 1.72, the values of λ(K,C), λ(K,N), λ(Na,C), and λ(Na,N) between nearest-neighbor ions along the c direction (see Fig. 4). As mentioned above, the value 1.72 was chosen to give us the best fit to a, b, and c. Physically, the repulsive force comes from the CN^- ion as a whole and not from the individual C and N atoms. In our model we approximate this repulsive force between *ions* with a sum of repulsive forces between *atoms*. This approximation works fine for most pairs of ions, but for the pairs shown in Fig. 4 where the positive ion is nearly equidistant from both the C and N atoms, the sum of repulsive forces between *atoms* is likely to give a resultant repulsive force between *ions* which is too large. Thus, in order to fit our model to the known structure parameters, we reduced λ_{ij} for these pair interactions by a factor 1.72.

As can be seen in Table IX, our fit to a, b, and c is fairly good. In fact, considering that the *same* set of force parameters [with the exception of λ(K,K),ρ(K,K) and λ(Na,Na),ρ(Na,Na), of course] are used for both KCN and NaCN, the agreement is remarkable.

Now let us examine the asymmetry between the C and N ends of the CN^- ion. This asymmetry is what gives rise to nonzero values of b_{anion} and b_{CN}. In our model the asymmetry can arise from two different sources: (1) the electric dipole moment p of the CN^- ion, and (2) a difference in the Born-Mayer parameters for the C and N atoms, i.e., the C atom is slightly "larger" than the N atom.

We found early in our investigation that both sources

TABLE IX. Best fit of our model to experimental data for the structure of KCN and NaCN in phase III. We used the same set of interatomic force parameters for both KCN and NaCN.

	Our model (Å)	Experimental (Å)
	KCN	
a	4.23	4.20
b	5.27	5.26
c	5.96	6.09
b_{anion}	0.18	0.05
b_{CN}	−0.04	0.04
	NaCN	
a	3.70	3.63
b	4.80	4.85
c	5.56	5.45
b_{anion}	0.18	0.1
b_{CN}	−0.02	0.00

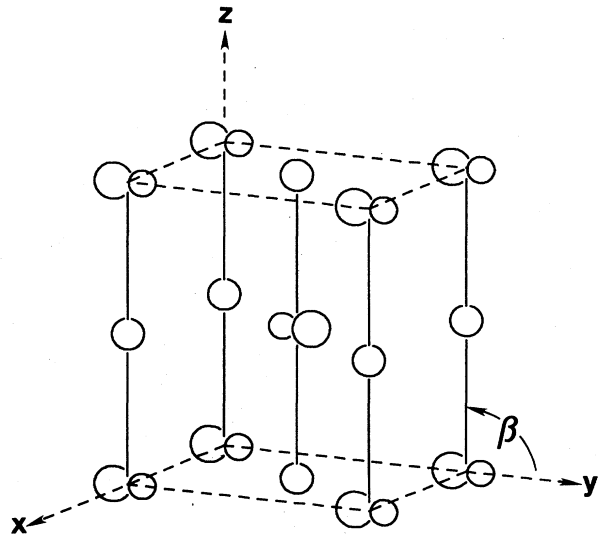

FIG. 4. Interactions between nearest-neighbor ions along the c axis as indicated by the solid lines. In our model the contribution of the Born-Mayer repulsive force to these interactions is reduced by a factor 1.72. Also, we add a phenomenological term to these interactions which results in a restoring torque on the CN^- ion to keep the angle β near 90°.

give rise to nearly the same effects. A difference in size of the C and N atoms gives rise to an ordering of the CN^- ions at low temperature just as well as a permanent dipole moment on the CN^- ion does. No permanent dipole moment of the CN^- ion is needed to explain the ordering phenomena! In reality, both effects (atomic size and dipole moment) are present and contribute to the ordering. We realized that we would not be able to separate these two effects in our model and thus decided to combine the C—N asymmetry into one parameter only: the dipole moment p. Accordingly, we removed the "size" asymmetry by choosing some average values $\lambda(C,C)=\lambda(N,N)$ and $\rho(C,C)=\rho(N,N)$, as shown in Table VIII. We do not intend to imply here that there is no "size" asymmetry present in KCN and NaCN. It is just more "convenient" to combine all the asymmetry into the dipole moment. We find that the principal results of our model do not depend on how we distribute the asymmetry effects between the dipole moment and the Born-Mayer parameters.

We did not try to fit our model to the experimental values of b_{anion} and b_{CN}. The experimental uncertainty in these values is nearly as large as the values themselves. Our choice of p is based on a fit to other experimental data, as will be discussed later.

B. Normal modes of vibration

Using our model we calculated the normal modes of vibration for the X structure in KCN and NaCN. In our calculations we used the harmonic approximation, essentially following the method briefly discussed in Ref. 22. From the calculation we found an unstable mode: an infrared-active mode involving rotations of the CN^- ions in the b-c plane. (Up to this point, we had constrained the displacements of the CN^- ion by symmetry and allowed only atomic displacements along the b direction.) The source of this instability is the lack of restoring force against the rotation of the CN^- ion in the b-c plane, especially when the neighboring CN^- ions also rotate in such a way that all the CN^- ions avoid each other. The fact that we had *reduced* the Born-Mayer repulsive force between the CN^- ion and its two neighboring positive ions in the $\pm c$ directions made this instability even worse.

We tried to eliminate the unstable mode by adjusting some of the already existing force parameters, but were unsuccessful. Thus we added to the energy U a phenomenological term which would provide the needed restoring force against this mode. This term involves an interaction between a CN^- ion and a neighboring positive ion in the c direction (see Fig. 4):

$$U_{ij}=\tfrac{1}{2}\alpha(\beta-\beta_0)^2\,, \tag{13}$$

where β is the angle between the C—N axis and a vector from the CN^- center of mass to the positive ion. We chose $\beta_0=\pi/2$. The parameter α was adjusted to fit our model to experimental Raman light-scattering data.[12,22] We obtained $\alpha=0.5\times10^{-12}$ erg for KCN and $\alpha=0.8\times10^{-12}$ erg for NaCN.

The Raman-active modes calculated from our model are shown in Table X and are compared with experimental data. Note that the modes polarized in the a-b plane do not depend on the value of α and thus contain *no* adjustable parameters. (The force parameters were already

TABLE X. Raman-active vibrational modes in KCN and NaCN. Results of our model are compared with experimental data from Refs. 12 and 22. The atomic displacements have arbitrary units. The intensity is given in relative units, using 1.0 for the most intense line.

			KCN				
	Our model					Experimental data	
	Frequency		Atomic displacements			Frequency	
Polarization	(cm^{-1})	K	Cn(c.m.)	CN(rot)	Intensity	(cm^{-1})	Intensity
a-b	68	13	11	5	0.08		
	123	4	−3	−31	1.0	121	1.0
	142	8	−16	9	0.06	165	0.04
b-c	108	14	3	13	0.23	113	0.02
	162	2	15	−20	0.25	132	0.59
	171	7	−12	−22	0.26	190	0.24

			NaCN				
	Our model					Experimental data	
	Frequency		Atomic displacements			Frequency	
Polarization	(cm^{-1})	Na	CN(c.m.)	CN(rot)	Intensity	(cm^{-1})	Intensity
a-b	88	15	13	5	0.05	88	0.02
	145	5	−1	−32	1.0	124	1.0
	172	14	−15	5	0.02	196	0.03
b-c	119	17	10	9	0.11	150	0.09
	203	6	−15	19	0.18	186	0.31
	236	10	−8	−25	0.22	252	0.71

adjusted to fit *other* experimental data.) With this consideration we see that the agreement between our model and experimental data is really quite good. On the other hand, the modes polarized in the a-c plane *do* depend strongly on the value of α. We adjusted α to give the best possible agreement with experimental data. This required a different value of α for KCN and NaCN. The inclusion of terms like Eq. (13) into the energy U did not have much effect on our fit of the force parameters to the crystal structure.

C. Elastic constants

The elastic constants are easily calculated from our model. For example, if we apply a stress X_x along the a axis, the equilibrium value of $\partial U/\partial a$ is no longer zero, but is given by

$$\frac{\partial U}{\partial a}=\tfrac{1}{2}NbcX_x \ . \tag{14}$$

The factor $\frac{1}{2}$ is included because there are two molecules per unit cell. To find the new equilibrium crystal structure, we solve Eq. (14) along with

$$\frac{\partial U}{\partial b}=\frac{\partial U}{\partial c}=\frac{\partial U}{\partial b_{\text{anion}}}=\frac{\partial U}{\partial b_{\text{CN}}}=0 \ , \tag{15}$$

and obtain new values a', b', c', b'_{anion}, and b'_{CN}. We can then calculate three strain components,

$$e_x=a'/a, \quad e_y=b'/b, \quad e_z=c'/c \ , \tag{16}$$

from which we can calculate the elastic compliance constants,

$$S_{11}=e_x/X_x, \quad S_{21}=e_y/X_x, \quad S_{31}=e_z/X_x \ . \tag{17}$$

Similarly, we can calculate six other elastic constants corresponding to stresses in the b and c directions. The result is shown in Table XI. The inverse of $\overleftrightarrow{S}$ gives us $\overleftrightarrow{C}$, the elastic stiffness tensor, which is also shown in Table XI. The compressibility κ is given by

$$\kappa=\sum_{i,j}S_{ij} \ , \tag{18}$$

and is also given in Table XI.

TABLE XI. Elastic stiffness tensor C, elastic compliance tensor S, and compressibility κ, calculated from our model for phase III of KCN and NaCN.

	KCN (10^{10} Pa)	NaCN (10^{10} Pa)
C_{11}	2.1	3.1
C_{22}	3.1	5.0
C_{33}	2.2	2.0
C_{12}	1.4	1.8
C_{23}	0.8	1.1
C_{13}	0.6	0.9
	(10^{-11} Pa^{-1})	(10^{-11} Pa^{-1})
S_{11}	6.7	4.3
S_{22}	4.6	2.6
S_{33}	5.1	5.9
S_{12}	−2.7	−1.3
S_{23}	−0.9	−0.9
S_{13}	−0.8	−1.1
κ	7.5	6.2

The elastic constants have not yet been measured experimentally in the low-temperature phase of KCN and NaCN. However, a nominal "C_{11}" was measured by Rehwald *et al.*[11] for KCN. They measured the "time of flight" for a longitudinal ultrasonic pulse along the [100] direction of the cubic phase I. At the phase transition from the cubic phase I to the orthorhombic phase II, a single crystal of KCN breaks up into 12 different kinds of domains.[51,9,7] The size of these domains[16] is approximately 80 μm. Thus, an ultrasonic pulse traveling through a macroscopic KCN crystal must, in general, pass through each of the 12 different kinds of domains many times. If we assume that the total distance traveled through any particular kind of domain is $\frac{1}{12}$ of the total distance traveled through the crystal (i.e., we assume that each kind of domain is equally distributed throughout the crystal), we can calculate the "average" time of flight from which we obtain an expression for the value of C_{11} measured by Rehwald *et al.*,

$$C_{11}=\left[\sum_{i=1}^{12}(\hat{r}_i\cdot\overleftrightarrow{C}\cdot\hat{r}_i)^{-1/2}\right]^{-2} \ , \tag{19}$$

where $\hat{r}_i$ is a unit vector along the direction of propagation of the pulse with respect to the crystal axes in domain type i. Using our values for $\overleftrightarrow{C}$ in Table XI, we obtain $C_{11}=21$ GPa, which agrees reasonably well with the experimental value $C_{11}=26$ GPa at about 60 K. Note that we have not included any kinetic considerations in our model. Inclusions of such motion would increase our value of C_{11} and bring it closer to the experimental value.

D. Phase II

In phase II the CN^- ions are disordered with respect to parallel and antiparallel alignment along the b axis. We applied our model to this phase by distributing the CN^- alignments randomly among the 108 molecules contained within a distorted cubic volume of dimensions

$$6(a^2+b^2)^{1/2}\times 6(a^2+b^2)^{1/2}\times 6c \ .$$

Periodic boundary conditions were used to eliminate any crystal surfaces. Relaxation of the ions to positions which give a minimum in U presented some challenges in the numerical calculations since we could not take advantage of symmetry in this phase.

The exact positions of individual ions at equilibrium are randomly distributed about an "average" position of symmetry. The lattice is locally disordered. Only on a macroscopic scale do we find the orthorhombic symmetry of space group D_{2h}^{25}. Evidence of such local disorder was seen in NMR data by Stokes, Case, and Ailion.[10] From the data, the rms angle θ_{rms} between the C—N axis and the macroscropic b axis was found to be 3.3° (this result

was revised slightly from the value given in Ref. 10 due to an improved value of the C—N distance in phase II).

In our model the local disorder arises from the asymmetry between the C and N ends of the CN^- ions. As explained in Sec. IV, we have combined all the asymmetry into the CN^- dipole moment p. Thus, the value of θ_{rms} obtained from our model is very sensitive to our choice for the value of p. We chose p so that our model would yield $\theta_{rms}=3.3°$, in agreement with the experimental data. This resulted in $p/e=0.11$ Å ($p=0.53$ D). This value is slightly larger than the various experimentally determined values[52–54] of p (they range from 0.3 to 0.5 D) for CN^- defects in alkali halide crystals. The theoretical value from finite-field calculations by Gready *et al.*[49] for a free CN^- ion is $p=0.37$ D. The value from a density-functional theory of LeSar and Gordon[25] is $p=0.22$ D in KCN and $p=0.24$ D in NaCN. We might expect our fitted value of p to be too large since it includes *all* sources of asymmetry in the CN^- ion, as discussed in Sec. IV.

VI. OTHER ORDERED STRUCTURES

We can now use the force constants determined for our model to investigate all six possible structures of phase III which are listed in Table VI. For each structure we arrange the orientation of the CN^- ions as described in Sec. III, and then let them relax to positions which give a minimum energy U for the crystal. The lattice angles α, β, and γ between the pairs of basis vectors $\vec{b}$-$\vec{c}$, $\vec{c}$-$\vec{a}$, and $\vec{a}$-$\vec{b}$, respectively, as well as the lengths a, b, and c of the basis vectors, are also allowed to vary. The resulting structures for KCN are shown in Table XII. The results for NaCN are similar. We can see from the table that the CN^- ions are displaced from their sites in such a way as to give the point symmetries listed in Table VI. From Table VI we also see that three of the structures (R, S, and T) are monoclinic. In agreement with this, we find in our model for KCN that $\beta=89.7°$ for the R structure, $\alpha=93.1°$ for the S structure, and $\gamma=89.8°$ for the T structure. In NaCN we find similar results. The values of a, b, and c also vary slightly (by a few hundredths of an angstrom) between the structures.

The energy per molecule, relative to that of the disordered phase II, is shown in Table XIII for each structure. For the ferroelectric Γ structure, an additional term is added to U for the interaction of ions with the electric field produced by the charge density at the boundary of the volume where the lattice summation is performed [see Eq. (5)]. The macroscopic polarization P in this case arises from both permanent dipole moments as well as *induced* dipole moments:

$$P=(2p+2q_0b_{CN})/abc\ . \tag{20}$$

TABLE XII. Atomic positions calculated from our model for the ordered structures of KCN. Similar results were obtained for NaCN. The CN^- and K sites are given for the D_{2h}^{25} structure of phase II in terms of $\vec{a}$, $\vec{b}$, and $\vec{c}$. The displacements of the atoms from these sites are given in angstroms along the $\vec{a}$, $\vec{b}$, and $\vec{c}$ directions. As shown, there is one molecule per primitive unit cell in the Γ structure, two molecules per cell in the R, S, and T structures, and four molecules per cell in the W structure.

	KCN				
		Displacement			Displacement
$\vec{k}$	CN^- site	C	N	K site	K
Γ	0,0,0	0,−0.51,0	0,0.69,0	$\frac{1}{2},\frac{1}{2},0$	0,0,0
X	0,0,0	0,−0.69,0	0,0.51,0	$\frac{1}{2},\frac{1}{2},0$	0,−0.18,0
	$\frac{1}{2},\frac{1}{2},\frac{1}{2}$	0,0.69,0	0,−0.51,0	$1,1,\frac{1}{2}$	0,0.18,0
R	0,0,0	0,−0.51,0	0,0.69,0	$\frac{1}{2},\frac{1}{2},0$	0,0,0
	$\frac{1}{2},\frac{1}{2},\frac{1}{2}$	0,0.51,0	0,−0.69,0	$1,1,\frac{1}{2}$	0,0,0
S	0,0,0	0,−0.58,−0.05	0,0.61,−0.17	$\frac{1}{2},\frac{1}{2},0$	0,0,0
	$\frac{1}{2},\frac{1}{2},\frac{1}{2}$	0,0.58,0.05	0,−0.61,0.17	$1,1,\frac{1}{2}$	0,0,0
T	0,0,0	−0.02,−0.62,0	0.00,0.58,0	$\frac{1}{2},\frac{1}{2},0$	−0.12,−0.01,0
	$\frac{1}{2},\frac{1}{2},\frac{1}{2}$	0.02,0.62,0	0.00,−0.58,0	$1,1,\frac{1}{2}$	0.12,0.01,0
W	0,0,0	0,−0.63,0	0,0.57,0	$\frac{1}{2},\frac{1}{2},0$	−0.13,0,0
	$\frac{1}{2},\frac{1}{2},\overline{\frac{1}{2}}$	0,−0.63,0	0,0.57,0	$1,1,\overline{\frac{1}{2}}$	−0.13,0,0
	0,0,1	0,0.63,0	0,−0.57,0	$\frac{1}{2},\frac{1}{2},1$	0.13,0,0
	$\frac{1}{2},\frac{1}{2},\frac{1}{2}$	0,0.63,0	0,−0.57,0	$1,1,\frac{1}{2}$	0.13,0,0

TABLE XIII. Relative energy per molecule calculated from our model for the possible structures of phase III. These values are relative to that of the disordered phase II, which we calculated to be 8.947×10^{-12} erg in KCN and 9.827×10^{-12} erg in NaCN. For comparison, the relative energies obtained by Pirc and Vilfan (Ref. 23) are also shown (these are *not* relative to phase II and depend on the magnitude of p).

	Our model		Model of Pirc and Vilfan	
	KCN	NaCN	KCN	NaCN
	$\Delta U/N$	$\Delta U/N$	$2\Delta U'/p^2N$	$2\Delta U'/p^2N$
$\vec{k}$	(10^{-15} erg)	(10^{-15} erg)	(nm^{-3})	(nm^{-3})
Γ	−2	−4	−74.1	−128.0
X	−16	−18	−96.7	−321.0
R	2	−1	−47.7	−115.0
S	16	24	38.6	43.0
T	−11	−14		
W	−10	−13		

The relative energies calculated from our model are in rough agreement with those calculated by Pirc and Vilfan[23] (see Table XIII. Note that the values of Pirc and Vilfan are *not* relative to that of phase II and also depend on the magnitude of p). Both our values and those of Pirc and Vilfan show the energy increasing as we go from the X to Γ to R to S structures. We see that our model shows a difference in energy between phase III (X structure) and phase II of about 3×10^{-14} erg/molecule for both KCN and NaCN. Calculations from other models[25] have yielded results which are slightly larger (ranging from 3×10^{-14} to 8×10^{-14} erg).

From our model we can see how induced dipoles at the positive-ion sites greatly affect the relative energy of the structure. In Table XII we find that the displacements of the K and Na ions are greatest in the X, T, and W structures. Thus the induced dipoles are greatest in those structures. In Table XIII we see that those structures have the lowest energies. The X structure, which exhibits the largest displacements of the K or Na ion, has the lowest energy, and thus is the structure most energetically favorable, in agreement with experiment.

ACKNOWLEDGMENTS

The authors are grateful for helpful discussions with Professor E. G. Larson, Professor D. L. Decker, and Professor J. D. Barnett.

[1]M. Julian and F. Lüty, Ferroelectrics **16**, 201 (1977); M. D. Julian, Ph.D. thesis, University of Utah, 1976.
[2]F. Lüty and J. Ortiz-Lopez, Phys. Rev. Lett. **50**, 1289 (1983).
[3]J. M. Rowe, J. J. Rush, and E. Prince, J. Chem. Phys. **66**, 5147 (1977).
[4]D. Fontaine, Ph.D. thesis, L'Université Pierre et Marie Curie, Paris, 1978; D. Fontaine, C. R. Acad. Sci., Ser. B **281**, 443 (1975).
[5]N. Nucker, K. Knorr, and H. Jex, J. Phys. C **11**, 1 (1978).
[6]J. P. von der Weid, L. C. Scavarda do Carmo, R. R. do Santos, B. Koiller, S. Costa Ribeiro, and A. S. Chaves, J. Phys. (Paris) Colloq. **12**, C7-241 (1976); J. P. von der Weid, L. C. Scavarda do Carmo, and S. Costa Ribeiro, J. Phys. C **12**, 4927 (1979).
[7]W. Buchheit, S. Elschner, H. D. Maier, J. Petersson, and E. Schneider, Solid State Commun. **38**, 665 (1981).
[8]D. E. O'Reilly, J. Chem. Phys. **58**, 3023 (1973); D. E. O'Reilly, E. M. Peterson, C. E. Scheie, and P. K. Kadaba, *ibid.* **58**, 3018 (1973).
[9]A. Tzalmona and D. C. Ailion, Phys. Rev. Lett. **44**, 460 (1980).
[10]H. T. Stokes, T. A. Case, and D. C. Ailion, Phys. Rev. Lett. **47**, 268 (1981).
[11]W. Rehwald, J. R. Sandercock, and M. Rossinelli, Phys. Status Solidi A **42**, 699 (1977).
[12]D. Durand, L. C. Scavarda do Carmo, A. Anderson, and F. Lüty, Phys. Rev. B **22**, 4005 (1980).
[13]L. C. Scavarda do Carmo, F. Lüty, T. Holstein, and R. Orbach, Phys. Rev. B **23**, 3186 (1981).
[14]D. Fontaine, J. Raman Spectrosc. **9**, 115 (1980).
[15]W. Dultz, J. Chem. Phys. **65**, 2812 (1976); W. Dultz, H. Krause, and L. W. Winchester, Jr., *ibid.* **67**, 2560 (1977).
[16]M. D. Julian and F. Lüty, Phys. Rev. B **21**, 1647 (1980).
[17]J. P. von der Weid and M. A. Aegerter, J. Phys. C **11**, 1505 (1978).
[18]M. Rossinelli, M. Bosch, and G. Zumofen, Phys. Rev. B **22**, 6403 (1980).
[19]R. R. dos Santos, B. Koiller, J. P. von der Weid, S. Costa Ribeiro, A. S. Chaves, and F. C. Sa Barreto, J. Phys. C **11**, 4557 (1978).
[20]D. K. Blat and V. I. Zinenko, Zh. Eksp. Teor. Fiz. **79**, 974 (1980) [Sov. Phys.—JETP **52**, 495 (1980)].
[21]A. J. Holden, V. Heine, J. C. Inkson, C. M. Varma, and M. A. Bosch, J. Phys. C **12**, 1035 (1979).
[22]A. Anderson, P. Gash, and F. Lüty, Phys. Status Solidi B **105**, 315 (1981).
[23]R. Pirc and I. Vilfan, Solid State Commun. **39**, 181 (1981).
[24]B. Koiller, M. A. Davidovich, L. C. Scavarda do Carmo, and F. Lüty, Phys. Rev. B **29**, 3586 (1984).
[25]R. LeSar and R. G. Gordon, J. Chem. Phys. **77**, 3682 (1982); I. R. McDonald, D. G. Bounds, and M. L. Klein, J. Phys. C **16**, 3217 (1983).
[26]J. M. Bijvoet and H. J. Verveel, Rec. Trav. Chim. Pays-Bas **54**, 631 (1935); H. J. Verveel and J. M. Bijvoet, Z. Kristallogr.

100 201 (1939).
[27]J. M. Bijvoet and J. A. Lely, Rec. Trav. Chim. Pays-Bas **59**, 908 (1940).
[28]H. Suga, T. Matsuo, and S. Seki, Bull. Chem. Soc. Jpn. **38**, 1115 (1965).
[29]T. Matsuo, H. Suga, and S. Seki, Bull. Chem. Soc. Jpn. **41**, 583 (1968).
[30]L. D. Landau and E. M. Lifshitz, *Statistical Physics,* 3rd ed. (Pergamon, Oxford, 1980), Pt. 1.
[31]J. L. Birman, Phys. Rev. Lett. **17**, 1216 (1966).
[32]F. E. Goldrich and J. L. Birman, Phys. Rev. **167**, 528 (1968).
[33]J. L. Birman, in *Group Theoretical Methods in Physics,* edited by P. Karmer and A. Rieckers (Springer, New York, 1978), pp. 203—222.
[34]M. V. Jarić and J. L. Birman, Phys. Rev. B **16**, 2564 (1977).
[35]M. V. Jarić, Phys. Rev. B **23**, 3460 (1981).
[36]M. V. Jarić, Phys. Rev. B **25**, 2015 (1982).
[37]C. J. Bradley and A. P. Cracknell, *The Mathematical Theory of Symmetry in Solids* (Oxford, London, 1972).
[38]*International Tables for X-Ray Crystallography,* edited by N. F. M. Henry and K. Lonsdale (Kynoch, Birmingham, U.K., 1965), Vol. I.
[39]E. Ascher, Helv. Phys. Acta **39**, 40 (1966); **39**, 466 (1966); Phys. Lett. **20**, 352 (1962).
[40]D. Mukamel and M. V. Jarić, Phys. Rev. B **29**, 1465 (1984).
[41]T. Matsuo, H. Suga, and S. Seki, Bull. Chem. Soc. Jpn. **41**, 583 (1968).
[42]F. G. Fumi and M. P. Tosi, J. Phys. Chem. Solids **25**, 31 (1964).
[43]T. L. Gilbert, J. Chem. Phys. **49**, 2640 (1968).
[44]K. V. Mirskaya, I. E. Kozlova, and V. F. Bereznitskaya, Phys. Status Solidi B **62**, 291 (1974).
[45]K. V. Mirskaya and V. V. Nauchitel, Kristallografiya **17**, 73 (1972) [Sov. Phys.—Crystallogr. **17**, 56 (1972)].
[46]D. Sahu and S. D. Mahanti, Phys. Rev. B **26**, 2981 (1982).
[47]M. P. Tosi, in *Solid State Physics,* edited by F. Seitz and D. Turnbull (Academic, New York, 1964), Vol. 16, p. 1.
[48]B. Carnahan, H. A. Luther, and J. O. Wilkes, *Applied Numerical Methods* (Wiley, New York, 1969), p. 319.
[49]J. E. Gready, G. B. Bacskay, and N. S. Hush, Chem. Phys. **31**, 467 (1978).
[50]D. G. Bounds, M. L. Klein, and I. R. McDonald, Phys. Rev. Lett. **46**, 1682 (1981).
[51]A. Cimino and G. S. Parry, Nuovo Cimento **19**, 971 (1961).
[52]H. S. Sack and M. C. Moriarty, Solid State Commun. **3**, 93 (1965); P. P. Peressini, J. P. Harrison, and R. O. Pohl, Phys. Rev. **182**, 939 (1969).
[53]W. D. Seward and V. Narayanamurti, Phys. Rev. **148**, 463 (1966).
[54]F. Holuj and F. Bridges, Phys. Rev. B **20**, 3578 (1979).